Journal of Composite Materials

http://jcm.sagepub.com

Analysis of a Stitched Double Cantilever Beam

Bhavani V. Sankar and Sreerama M. Dharmapuri

Journal of Composite Materials 1998; 32; 2203
DOI: 10.1177/002199839803202402

The online version of this article can be found at:
http://jcm.sagepub.com/cgi/content/abstract/32/24/2203

Published by:
SAGE
http://www.sagepublications.com

On behalf of:
American Society for Composites

Additional services and information for *Journal of Composite Materials* can be found at:

Email Alerts: http://jcm.sagepub.com/cgi/alerts

Subscriptions: http://jcm.sagepub.com/subscriptions

Reprints: http://www.sagepub.com/journalsReprints.nav

Permissions: http://www.sagepub.co.uk/journalsPermissions.nav

Citations http://jcm.sagepub.com/cgi/content/refs/32/24/2203

Downloaded from http://jcm.sagepub.com at UNIV OF FLORIDA Smathers Libraries on May 26, 2009

Analysis of a Stitched Double Cantilever Beam

BHAVANI V. SANKAR* AND SREERAMA M. DHARMAPURI
Department of Aerospace Engineering
Mechanics & Engineering Science
Center for Studies of Advanced Structural Composites
P. O. Box 116250
231 Aerospace Building
University of Florida
Gainesville, FL 32611-6250

(Received September 8, 1997)
(Revised November 21, 1997)

ABSTRACT: A simple analytical model is presented to describe crack propagation in stitched laminated Double Cantilever Beam (DCB) specimens. The stitches are smeared and modeled as continuous cohesive springs, which are assumed to be linear-elastic until final failure. Timoshenko beam theory is used to model the DCB specimen. As the specimen is loaded, the stitches are assumed to break when the strain in the stitches reaches the ultimate strain. The crack tip is assumed to advance as the energy release rate at the crack tip reaches the Mode I fracture toughness of the parent laminate. A closed form solution is obtained for the problem of beam on elastic foundation and it is used to simulate the DCB test and crack propagation. Results presented include, load-deflection diagrams, crack bridging length and apparent fracture toughness for various stitch parameters. A semi-empirical formula is derived for the bridging length as a function of the stitch ultimate strain and fracture toughness of the parent laminate. The results are compared with experimental results. It is found that, for the case with Kevlar stitches, the linear elastic model of the stitch yarn is not adequate. It is shown that inelastic behavior of the stitches plays a significant role in increasing the fracture toughness due to stitching.

KEY WORDS: crack bridging, delamination, Double Cantilever Beam, laminated composites, Mode I fracture toughness, stitching, translaminar reinforcements.

*Author to whom correspondence should be addressed.

0021-9983/98/24 2203–23 $10.00/0
© 1998 Technomic Publishing Co., Inc.

Downloaded from http://jcm.sagepub.com at UNIV OF FLORIDA Smathers Libraries on May 26, 2009

from the SAGE Social Science Collections. All Rights Reserved.

1. INTRODUCTION

LAMINATED FIBER COMPOSITES that lack through-the-thickness reinforcements have poor interlaminar strength and fracture toughness. Translaminar reinforcement can be provided by inserting pins in the thickness direction (z-pinning) of the laminate or by stitching the layers with suitable yarns before resin impregnation. A number of experimental studies have shown that stitching can be effective in containing free edge delamination [1,2,3] and improving Mode I fracture toughness [2,3,4], Mode II fracture toughness [3] and Compression After Impact Strength [2,4]. Recently, there has been interest in modeling the effects of stitching. Mai and his coworkers [4] have developed analytical models to predict the effects of stitching on Mode I, Mode II and sublaminate buckling behavior. A comprehensive review of effects of stitching on delamination can be found in Dransfield et al. [5]. Jain and Mai [4] used a micromechanical approach in conjunction with the beam theory to study stitched DCB specimens. They developed a simple force-displacement relation for the stitch, and used the information to predict the crack growth resistance. Chen et al. [6] used a plane strain finite element model to study the effects of stitching. They introduced the concept of overstep length and its role in calculating effective strain energy release rate of the stitched composite.

In this paper, we propose a simple model for studying the load-deflection behavior and apparent fracture toughness of stitched DCB specimens. The stitches are smeared over the entire delaminated interface and modeled as linear cohesive springs (Winkler type elastic foundation). Thus, the load-deflection relationship of the stitch is linear. It is assumed that the stitches break when the strain in them reaches an ultimate value ε_u. Further, we assume that the stitches debond completely from the surrounding material before they become effective and hence, their length is equal to the laminate thickness $2h$, where h is the thickness of the sublaminate—either top or bottom—of the DCB specimen. The crack propagation is assumed to be in the same plane throughout the process. The modeling of stitches as an elastic foundation needs some justification. In reality, as the delamination propagates past the stitches, the stitches will debond from the surrounding composite. If they do not, then the stitches will possess infinite axial stiffness because of their infinitesimally small length. This will cause severe stress concentration, which will result in debonding of the stitches. As the stitches debond their stiffness will reduce relieving the interfacial shear stresses. We assume that this debonding is instantaneous and complete through the thickness of the laminate.

The smearing of the stitches as a continuous elastic foundation will yield good results as long as the crack propagation length and the crack bridging length are significantly larger than the stitch spacing. Further, elastic foundation models allow closed-form solutions that will help to understand the effects of various stitch parameters on the apparent fracture toughness, crack bridging length and load-deflection behavior of the DCB specimens.

Downloaded from http://jcm.sagepub.com at UNIV OF FLORIDA Smathers Libraries on May 26, 2009

2. ANALYTICAL MODEL

We propose to use the Timoshenko beam theory to determine the deflections and also the force and moment resultants in a stitched DCB specimen. Then, from the deflections we can determine the forces in the stitches. We shall also derive a method for computing the strain energy release rate (SERR) at the crack tip from the force and moment resultants acting on the beam. The problem we need to solve is depicted in Figure 1. However, it is sufficient to solve the modified problem as shown in Figure 2. In Figure 2, we consider only one half of the beam (top portion) because of symmetry. The beam is fixed at the right end, and a transverse force F and a couple C act at the left end. The stitches that bridge the crack are modeled as an elastic foundation which is described by the smeared stiffness k. The unit of k is force/length^3. The foundation constant k can be related to stitch parameters as:

$$k = N\frac{A_s E_s}{h} \tag{1}$$

where, A_s and E_s are the cross-sectional area and Young's modulus of the stitch, respectively, and N is the number of stitches per unit area of the laminate.

Let $w(x)$ be the transverse deflection and $\psi(x)$, the rotation of the beam. Upward deflection and clockwise rotation are considered positive. The constitutive relations of the beam are:

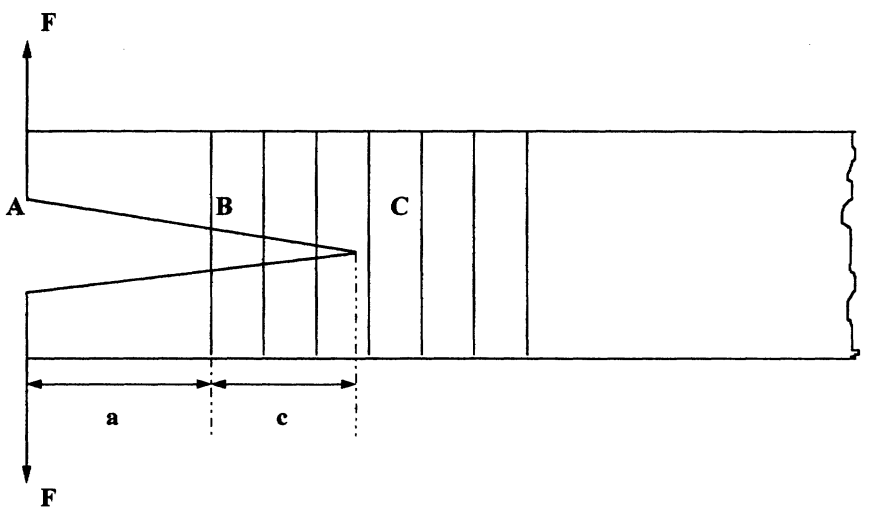

Figure 1. *Typical Stitched Double Cantilever Beam specimen.*

Downloaded from http://jcm.sagepub.com at UNIV OF FLORIDA Smathers Libraries on May 26, 2009

$$EI\frac{d\psi}{dx} = M(x) \tag{2}$$

$$GA\left(\psi + \frac{dw}{dx}\right) = V(x) \tag{3}$$

where, EI and GA are the effective flexural stiffness and transverse shear stiffness of the laminate, modeled as a homogeneous beam; M and V are the bending moment and shear force resultants at a given cross section. We assume that the shear correction factor is included in transverse shear stiffness. The equilibrium equations of the beam can be easily derived by considering the free body diagram of a small segment of the beam as:

$$\frac{dV}{dx} = kbw \tag{4}$$

$$\frac{dM}{dx} = V \tag{5}$$

where, b is the beam width. By substituting constitutive Equations (2) and (3) into Equations (4) and (5), the equilibrium equations can be expressed in terms of deflection and rotation as:

$$EI\frac{d^2W}{dx^2} - GA\psi - GA\frac{dw}{dx} = 0 \tag{6}$$

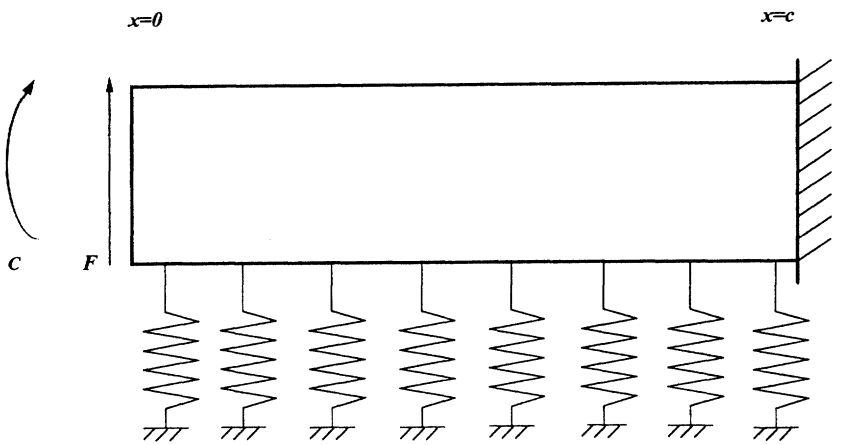

Figure 2. *Analytical model of DCB.*

Downloaded from http://jcm.sagepub.com at UNIV OF FLORIDA Smathers Libraries on May 26, 2009

$$GA = \frac{d\psi}{dx} + GA\frac{d^2w}{dx^2} - kbw = 0 \tag{7}$$

Let us assume solutions of the form:

$$\psi(x) = \sum_{i=1}^{4} a_i e^{\lambda_i x} \tag{8}$$

$$w(x) = \sum_{i=1}^{4} b_i e^{\lambda_i x} \tag{9}$$

By substituting the solutions from Equations (8) and (9) into the governing Equations (6) and (7) we obtain the roots of the characteristic equation:

$$\lambda_{1,2,3,4} = \pm\sqrt{\frac{\frac{k}{GA} \pm \sqrt{\frac{k^2}{(GA)^2} - \frac{4k}{EA}}}{2}} \tag{10}$$

and the ratio of the coefficients a_i and b_i as:

$$r_i = \frac{a_i}{b_i} = \frac{GA\lambda_i}{EI\lambda_i^2 - GA} \tag{11}$$

In addition to Equation (11) we need four boundary conditions to determine a_i and b_i. The boundary conditions at $x = 0$ are:

$$V = GA\left(\psi + \frac{dw}{dx}\right) = -F \tag{12a}$$

$$M = EI\frac{d\psi}{dx} = -C \tag{12b}$$

The boundary conditions at the right end $x = c$ are:

$$w = 0; \quad \psi = 0 \tag{13}$$

By substituting the solution given in Equations (8) and (9) and also using the relation in Equation (11) in the boundary conditions (12) and (13) we obtain a set of

Downloaded from http://jcm.sagepub.com at UNIV OF FLORIDA Smathers Libraries on May 26, 2009

linear equations in the coefficients $a_1, \ldots a_4$, which are given in Appendix I. Once the coefficients are determined, the solution of the problem depicted in Figure 2 is complete. Obtaining the deflection curve, stitch forces and the shear force and bending moment resultants at any cross section is a matter of straight forward calculation. The distributed stitch force at any location x is given by $kbw(x)$, and it acts downward the top half of the beam. It may be noted that the roots λ_i may be complex, depending on the beam properties EI and GA, and the stitch stiffness k. Hence, we used complex notations in the computer program used in the present study.

3. CRACK PROPAGATION CRITERION

As the DCB specimen is loaded the crack tip will advance leaving the stitches behind generating bridging length. The crack bridging is shown in Figure 1. The actual crack tip where the delamination ends is shown in the figure as C. Thus the delamination or crack length is denoted by $(a + c)$, where a is the distance from the loading point A to the first unbroken stitch B, and c is bridging length (length BC). We assume that both a and c continuously vary as the loading is increased. We have to define criteria for the crack propagation, i.e., the advancement of the crack tip, as well as for the stitches to break. The latter is quite straight forward and simple. We assume, that the stitches will break as the strain in them exceed a certain ultimate strain, ε_u. The crack tip C will propagate when the strain energy release rate (SERR) reaches a critical value, G_{Ic}, of the composite material system. This value of G_{Ic} will be, in general, different from that measured using a DCB test of the unstitched specimen, because, now the crack has to go around the stitches and also the effective area of delamination has been reduced by the area of cross section of the stitches. The actual effects can only be analyzed and understood using rigorous micromechanics of stitch debonding and propagation of delamination around the stitches. However, in this paper we tacitly assume that the G_{Ic} includes the effects discussed above. The next step is to devise a method to compute G_I. Then we can postulate that the crack will propagate when $G_I > G_{Ic}$.

In the present study, we use the method developed by Sankar [7] for composite beams, and later extended to composite plates by Sankar and Sonik [8]. In this method, the SERR of a beam like structure, is simply the difference between strain energy densities behind the crack tip and ahead of the crack tip. In the context of beam, the strain energy density refers to strain energy per unit length of the beam, which is given by:

$$U_L = \frac{1}{2}\left(\frac{M^2}{EI} + \frac{V^2}{GA} + \frac{P^2}{EA}\right) \tag{14}$$

Downloaded from http://jcm.sagepub.com at UNIV OF FLORIDA Smathers Libraries on May 26, 2009

where, M, V and P are the bending moment, shear force and axial force resultants, respectively. In the case of DCB specimens, $P \equiv 0$. Further, $U_L \equiv 0$ ahead of the crack tip as the force and moment resultants are zero. Accounting for the top and bottom laminates, the expression for SERR takes the form:

$$G_I = \frac{1}{b}\left(\frac{M^2}{EI} + \frac{V^2}{GA}\right) \tag{15}$$

where, M and V are the moment and force resultants just behind the crack tip, which can be easily calculated using the constitutive relations (2) and (3) and the solution for $w(x)$ and $\psi(x)$ given in Equations (8) and (9).

4. NUMERICAL SIMULATION OF THE DCB TEST

In this section, we shall describe the application of the methods described in Sections 2 and 3, analytical model and crack propagation criterion respectively in simulating the DCB test of a stitched specimen. We assume, that the test is conducted under displacement control mode. At any given instance let δ be the deflection of one ligament of the DCB specimen at the point of application of force, and let the first unbroken, stitch be at a distance a from the loading point and c, the bridging length. We apply a unit transverse force ($F = 1$) to the beam. We use the solution derived in Section 2 to find the maximum deflection of the stitches and also M and V behind the crack tip. The boundary conditions of Equation (12) become

$$\begin{aligned} M(0) &= -Fa \\ V(0) &= -F \end{aligned} \tag{16}$$

The maximum stitch deflection corresponds to $w(0)$, and the maximum strain in the stitch is then, $w(0)/h$. We shall denote the results due to the unit force with a 0 subscript. Thus, due to the unit force, the maximum stitch strain is ε_{m0}, the SERR at the crack tip is G_{I0} and the deflection of the beam at the load point is δ_0. The deflection, δ_0, refers to the deflection on one side of the beam—either top or bottom—and can be derived as:

$$\delta_0 = w_0(0) + \left(\psi_0(0) - \frac{1}{GA}\right)a + \frac{1.a^3}{3EI} + \frac{1.a}{GA} \tag{17}$$

In Equation (17), the terms on the right side respectively correspond to: deflection

Downloaded from http://jcm.sagepub.com at UNIV OF FLORIDA Smathers Libraries on May 26, 2009

at the first stitch location (point B in Figure 1) due to the unit force, tip deflection due to the slope at point B, cantilever beam deflection of the portion AB due to the unit force and additional deflection due to shear deformation of the beam AB. Having calculated all the required quantities for a unit force, we can scale them to a given deflection δ at the tip. Thus, we obtain for a given deflection δ:

$$F = \frac{\delta}{\delta_0}$$

$$\varepsilon_m = F\varepsilon_{m0} \tag{18}$$

$$G_I = F^2 G_{I0}$$

If $\varepsilon_m > \varepsilon_u$, then the stitches are allowed to break thus extending a to $a + \Delta a$, and reducing c to $c - \Delta a$, where, Δa and Δc are some incremental lengths used in the numerical simulation. If $G_I > G_{Ic}$ then, the crack is advanced by Δc and thus, c becomes $c + \Delta c$. Thus, for a given deflection δ, the force F, maximum strain in the stitch ε_m, bridging length c, and the SERR G_I, are calculated. In the next cycle, the deflection of the beam is increased to $\delta + \Delta\delta$, and the aforementioned calculations are repeated. The steps in the numerical simulation are depicted in the flow-chart in Figure 3. The results are plotted in the form of load-deflection curve (2δ vs. F; note that the total defection between the two ligaments of the DCB is 2δ). The calculation of the apparent fracture toughness G_{Ic-app}, is as follows. At any point on the load-deflection curve, we assume, that the unloading curve will be a straight line to the origin. We assume, that there is no permanent deformation of the beam and all deformations including that of the stitches are elastic. The work done ΔW is the area enclosed by the loading-unloading curves. The crack extension area ΔA is given by

$$\begin{aligned} \Delta A &= b(a + c - a_0 - c_0) \\ &= b\Delta l \end{aligned} \tag{19}$$

where, Δl is the crack extension, a_0 and c_0 are the initial values of a and c, respectively. The apparent fracture toughness is given by

$$G_{IC-app} = \frac{\Delta W}{\Delta A} \tag{20}$$

The maximum attainable apparent fracture toughness G_{Ic-max} can be derived by us-

Downloaded from http://jcm.sagepub.com at UNIV OF FLORIDA Smathers Libraries on May 26, 2009

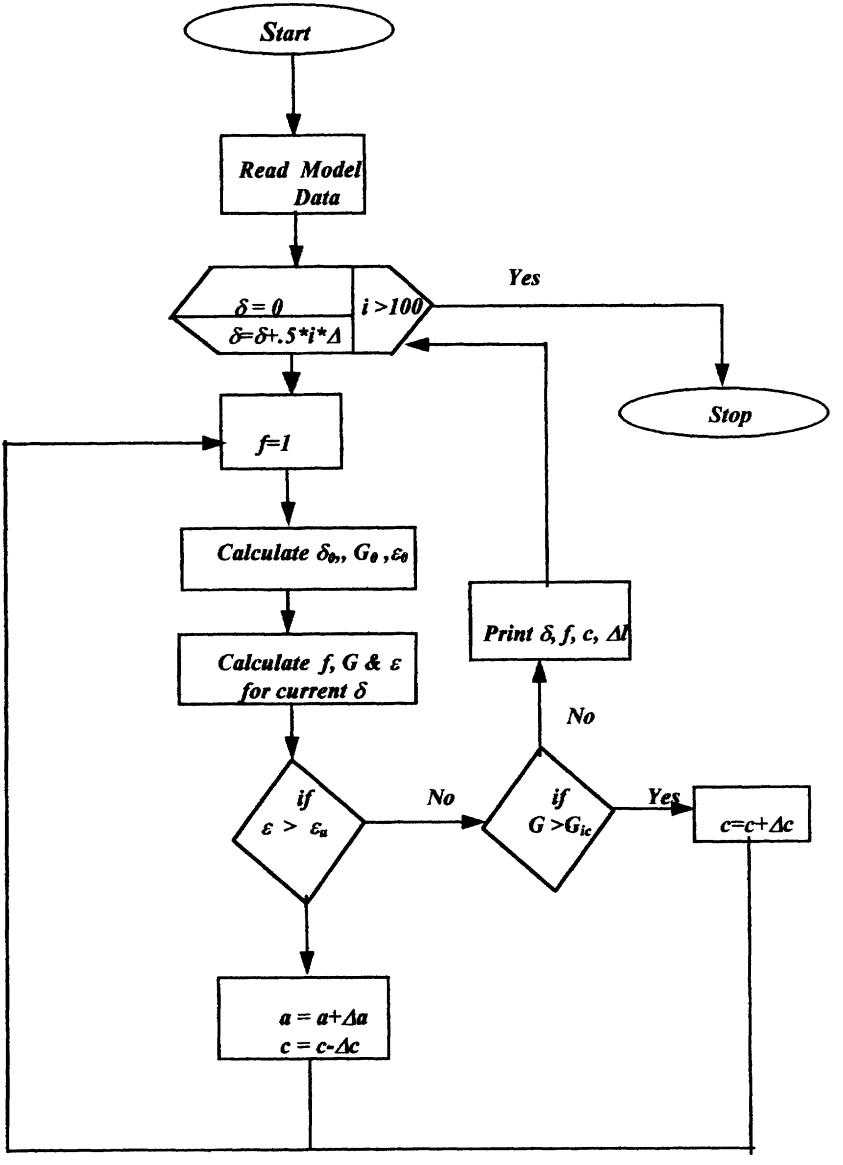

Figure 3. *Flowchart for crack propagation criteria.*

Downloaded from http://jcm.sagepub.com at UNIV OF FLORIDA Smathers Libraries on May 26, 2009

ing the energy approach. When the stitches break the maximum energy stored in one stitch U_{max} is given by

$$U_{max} = \left(\frac{1}{2} E_s \varepsilon_u^2\right)(2A_s h) \tag{21}$$

where, the terms in the first set of parentheses, represent the strain energy density in the stitch at the instant of failure, and the quantity in the second set of parentheses is equal to the volume of a single stitch. If N is the number of stitches per unit area, then, the maximum obtainable apparent fracture toughness can be derived as:

$$G_{Ic-max} = G_{Ic} + NU_{max} \tag{22}$$

Substituting the U_{max} from Equation (20) into Equation (21) we obtain,

$$G_{Ic-max} = G_{Ic} + A_f E_s h \varepsilon_u^2 \tag{23}$$

where, $A_f = NA_s$ can be defined as the areal fraction of stitches in the laminate.

5. NONDIMENSIONAL PARAMETERS

Since a large number of parameters are involved in describing the stitches and the laminated beam, it will be convenient to introduce a set of nondimensional parameters to present the results—especially, the effects of stitch parameters in increasing the apparent fracture toughness of the beam. The length dimension is normalized with respect to the laminate thickness h, and all the stiffness terms, e.g., Young's modulus and Shear modulus, are normalized by the equivalent beam Young's modulus, E_b, which can be calculated from the relation

$$(EI)_{eq} = \frac{E_b b h^3}{12} \tag{24}$$

Thus, the laminate thickness and Young's modulus will be equal to unity in all the cases considered. The other nondimensional parameters are described in Table 1. The range of numerical values of these parameters used in numerical simulations are presented in Table 2.

6. RESULTS AND DISCUSSION

This section is divided as: (a) verification of the our method of computing $\overline{G_I}$;

Downloaded from http://jcm.sagepub.com at UNIV OF FLORIDA Smathers Libraries on May 26, 2009

Table 1. Nondimensional variables.

Parameter Description	Nondimensional Parameter	Relation to Real Variables
Beam shear modulus	$\bar{G}_b$	$\frac{G_b}{E_b}$
Distance between the loading point and the first unbroken stitch	$\bar{a}_0, \bar{a}$	$\frac{a_0}{h}, \frac{a}{h}$
Bridging length	$\bar{c}_0, \bar{c}$	$\frac{c_0}{h}, \frac{c}{h}$
Young's modulus of the stitch yarn	$\bar{E}_s$	$\frac{E_s}{E_b}$
Foundation spring constant	$\bar{k}$	$\frac{kh}{E_b} = A_f \bar{E}_s$
Beam deflections	$\bar{\delta}, \bar{w}$	$\frac{\delta}{h}, \frac{w}{h}$
Force	$\bar{F}$	$\frac{F}{E_b bh} = \frac{F}{E_b h^2}$
Strain Energy Release Rate (SERR)	$\bar{G}_I$	$\frac{G_I}{E_b h}$
Maximum attainable apparent fracture toughness	$\bar{G}_{Ic-max}$	$\frac{G_{Ic-app}}{G_{Ic}} = 1 + \frac{\bar{k}\bar{\varepsilon}_u^2}{\bar{G}_{Ic}}$

Table 2. Range of values of variables used in program.

Nondimensional Parameter	Range of Values
$\bar{a}_0$	10
$\bar{c}_0$	0.1
$\bar{G}_b$	0.05
$\Delta\bar{a}, \Delta\bar{c}$	0.001
$\bar{k}$	10^{-7}–10^{-3}
$\bar{\varepsilon}_u$	0.005, 0.01, 0.05, 0.1
$\bar{G}_{Ic}$	10^{-7}–10^{-4}

Downloaded from http://jcm.sagepub.com at UNIV OF FLORIDA Smathers Libraries on May 26, 2009

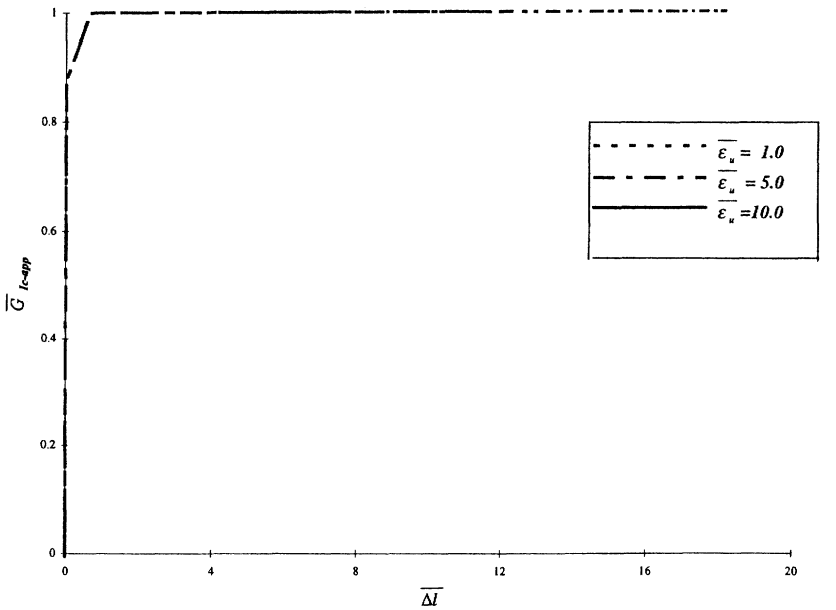

Figure 4. *Verification of method of calculating SERR (curves corresponding to all strains coalesce).*

(b) effect of varying $\overline{\varepsilon}_u$, $\overline{k}$, and $\overline{G}_{Ic}$ on the load-deflection diagrams, bridging length and apparent fracture toughness; and (c) comparison with experimental results.

6.1 Verification of the Method for Computing SERR

In order to verify our method of computing the SERR at the delamination front using Equation (15), we considered a case with very high $\overline{\varepsilon}_u$, so that the stitches would not break, but the crack would propagate. Thus, there should not be any increase in the apparent fracture toughness G_{app}. In Figure 4, the nondimensional $\overline{G}_{Ic-app}$ is plotted as a function of crack extension for various values of $\overline{\varepsilon}_u$ It can be seen from Figure 4 that as the crack propagates the nondimensional $\overline{G}_{Ic-app}$ (G_{app}/G_{Ic}) remains at unity for carious values of stitch ultimate strain. This validates Equation (15) for computing G_I for a stitched laminate.

6.2 Effect of Stitch Ultimate Strain

The effect of increasing the breakage strain of stitches on the load deflection behavior is shown in Figure 5. It may be noted, that the stitch strength does not have

Downloaded from http://jcm.sagepub.com at UNIV OF FLORIDA Smathers Libraries on May 26, 2009

any significant effect on the load at which the delamination begins to propagate. This is indicated by the fact that the initial load drop occurs at the same load for all cases. However after the crack propagates and stitches come into effect via debonding and crack bridging, the load for a given deflection is higher in the case of strong stitches, i.e., stitches with higher strain to break.

In Figure 6, the bridging length $\bar{c}$ is plotted as a function of crack extension, $\overline{\Delta l}$, for stitches with various strain to failure. The effect of ultimate strain of stitches is, in general, to increase the crack bridging length. An equation relating $\bar{c}$ and $\bar{\varepsilon}_u$ is presented at the end of this section. The apparent fracture toughness also increases with stitch ultimate strain as presented in Figure 7 but there is no apparent increase in $\overline{G}_{Ic}$ for small values of $\bar{\varepsilon}_u$ (e.g., $\bar{\varepsilon}_u = 0.005, 0.01$).

6.3 Effect of Stitch Stiffness

The effect of stitch stiffness on the DCB behavior was very much dependent on the $\overline{G}_{Ic}$ of the laminate. For higher values of $\overline{G}_{Ic}$ ($10^{-6} < \overline{G}_{Ic} < 10^{-4}$) considered, there was no significant change in the load deflection behavior, crack bridging length and the apparent fracture toughness due to changes in $\bar{k}$. When the value of $\overline{G}_{Ic}$ was reduced ($\overline{G}_{Ic} = 10^{-7}$), the effects of $\bar{k}$ could be realized as shown in Figures

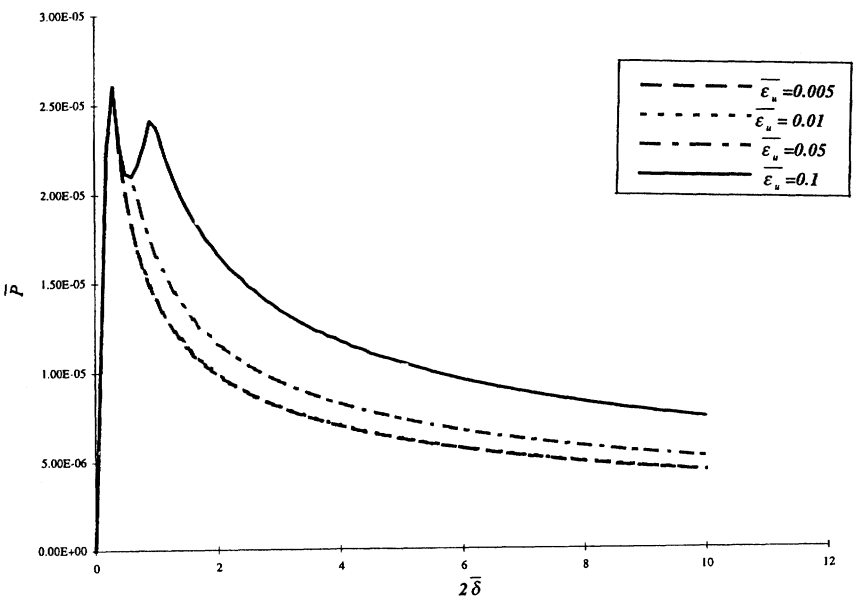

Figure 5. *$\bar{P}-2\bar{\delta}$ plot with varying $\bar{\varepsilon}_u$, $\overline{G}_{Ic} = 10^{-6}$, $\bar{k} = 10^{-4}$ (curves corresponding to $\bar{\varepsilon}_u$ = 0.005 and 0.01 coalesce).*

Downloaded from http://jcm.sagepub.com at UNIV OF FLORIDA Smathers Libraries on May 26, 2009

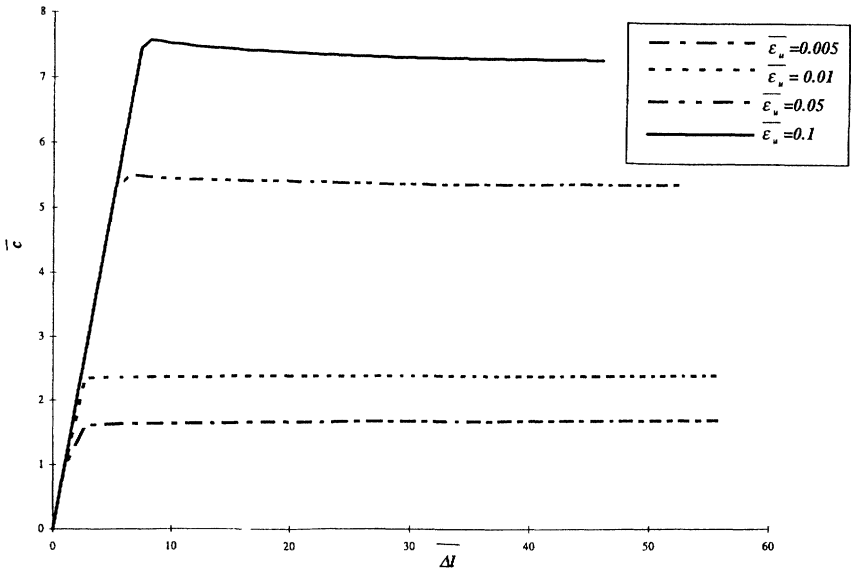

Figure 6. *$\bar{c} - \overline{\Delta l}$ plot with varying $\bar{\varepsilon}_u$, $\bar{G}_{Ic} = 10^{-6}$, $\bar{k} = 10^{-4}$.*

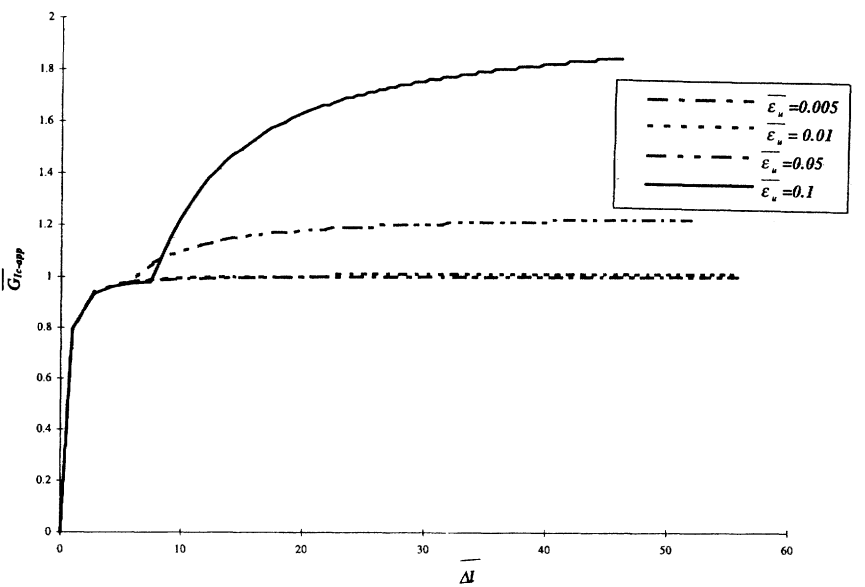

Figure 7. *$\bar{G}_{Ic-app} - \overline{\Delta l}$ plot with varying $\bar{\varepsilon}_u$, $\bar{G}_{Ic} = 10^{-6}$, $\bar{k} = 10^{-4}$.*

Downloaded from http://jcm.sagepub.com at UNIV OF FLORIDA Smathers Libraries on May 26, 2009

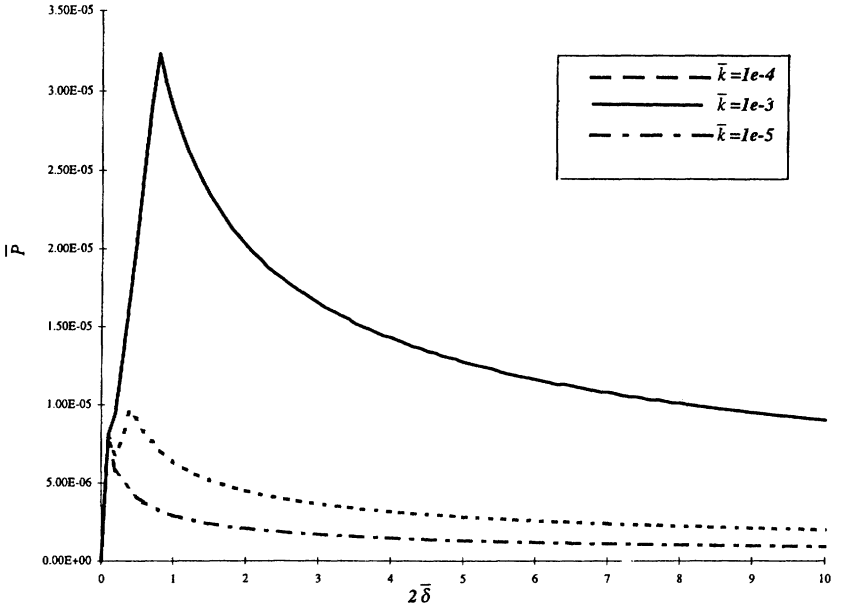

Figure 8. *$\bar{P}-2\bar{\delta}$ plot with varying $\bar{k}$, $\bar{G}_{Ic} = 10^{-7}$, $\bar{\varepsilon}_u = 0.05$.*

8 through 10. The crack begins to propagate initially at the same load level, as shown in Figure 8, but the load attains a second peak for higher $\bar{k}$, thus increasing the load carrying capacity of the beam. The bridging length $\bar{c}$ decreases with increase in stitch stiffness as presented in Figure 9. The apparent fracture toughness increases with $\bar{k}$, see Figure 10.

6.4 Effect of Fracture Toughness of the Parent Laminate

Obviously the higher the value of $\bar{G}_{Ic}$, the greater the load at which the delamination begins to propagate as in Figure 11. The load, for a given deflection, increases with increasing $\bar{G}_{Ic}$. From, Figure 12, it may be noted that increase in $\bar{G}_{Ic}$, decreases the bridging length. But the nondimensional apparent fracture toughness G_{Ic-app} decreases with increase in $\bar{G}_{Ic}$, indicating the stitches are not as effective in increasing the fracture toughness in laminates, that already have higher fracture toughness as shown in Figure 13.

6.5 Relationship among $\bar{c}$, $\bar{\varepsilon}_u$ and $\bar{G}_{Ic}$

The effects of snitch parameters on the bridging length is summarized in the log-log plots of Figure 14 and Figure 15. It was found that $\bar{c}$ is independent of $\bar{k}$ for

Downloaded from http://jcm.sagepub.com at UNIV OF FLORIDA Smathers Libraries on May 26, 2009

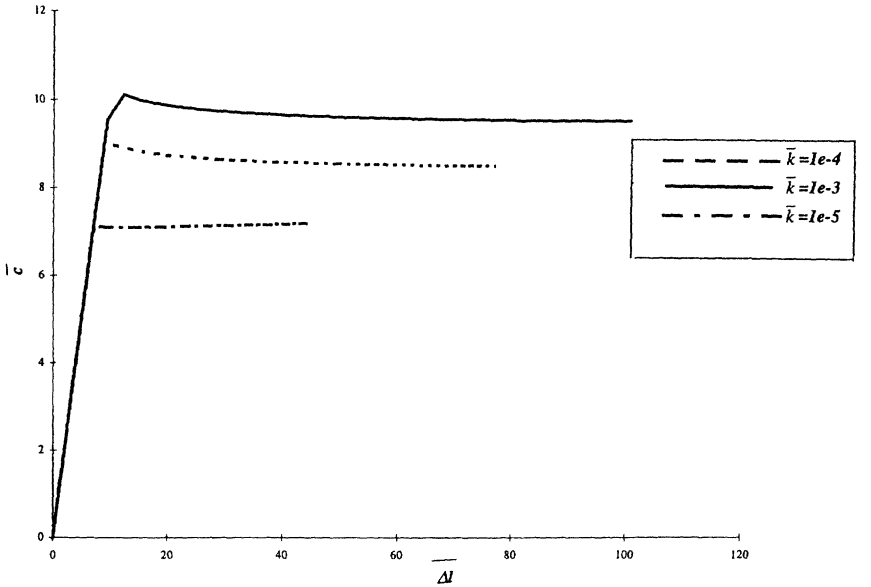

Figure 9. *$\bar{c} - \overline{\Delta l}$ plot with varying $\bar{k}$, $\bar{G}_{Ic} = 10^{-7}$, $\bar{\varepsilon}_u = 0.05$*

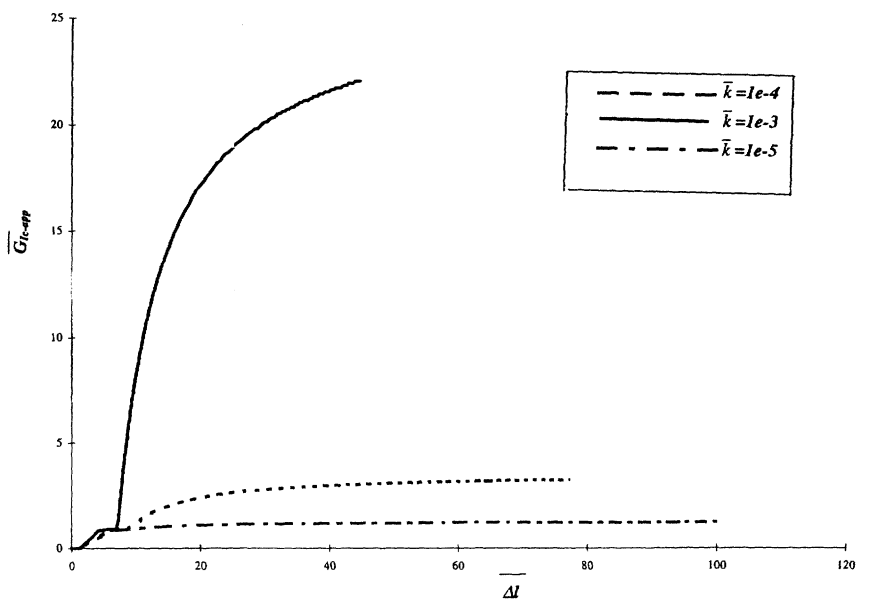

Figure 10. *$\overline{G}_{Ic-app} - \overline{\Delta l}$ plot with varying $\bar{k}$, $\bar{G}_{Ic} = 10^{-7}$, $\bar{\varepsilon}_u = 0.05$*

Downloaded from http://jcm.sagepub.com at UNIV OF FLORIDA Smathers Libraries on May 26, 2009

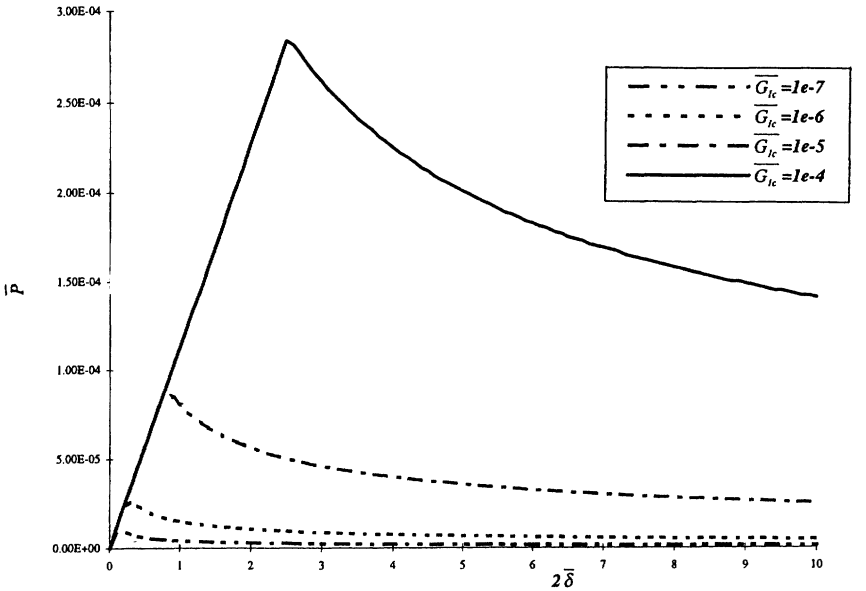

Figure 11. *$\bar{P} - 2\bar{\delta}$ plot with varying $\bar{G}_{Ic}$, $\bar{k} = 10^{-3}$, $\bar{\varepsilon}_u = 0.01$.*

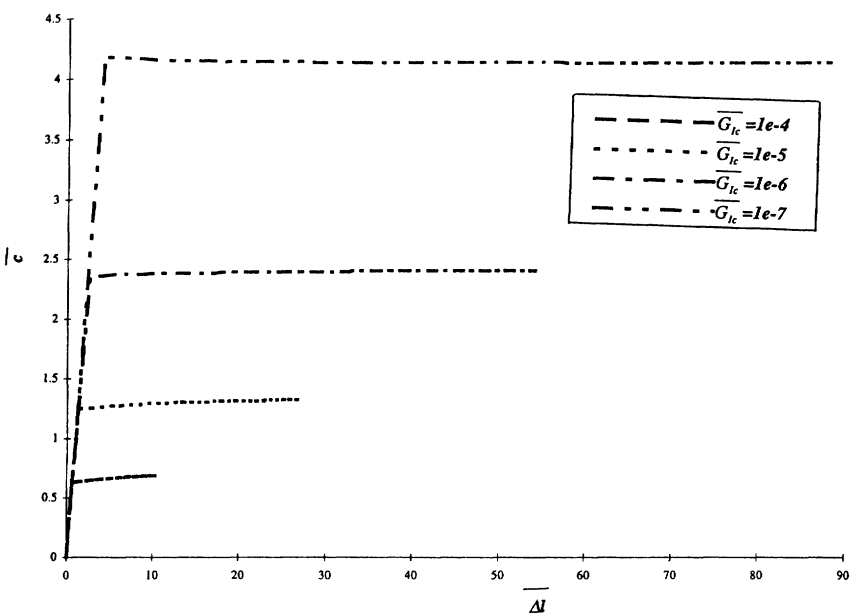

Figure 12. *$\bar{c} - \overline{\Delta l}$ plot with varying $\bar{G}_{Ic}$, $\bar{k} = 10^{-3}$, $\bar{\varepsilon}_u = 0.01$.*

Downloaded from http://jcm.sagepub.com at UNIV OF FLORIDA Smathers Libraries on May 26, 2009

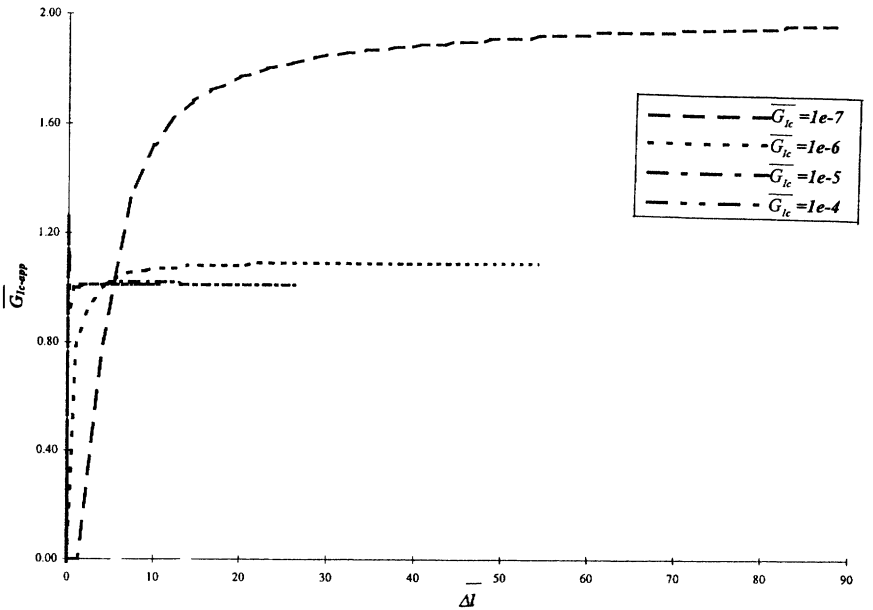

Figure 13. *$\overline{G}_{Ic-app} - \overline{\Delta l}$ plot with varying $\overline{G}_{Ic}$, $\bar{k} = 10^{-3}$, $\bar{\varepsilon}_u = 0.01$.*

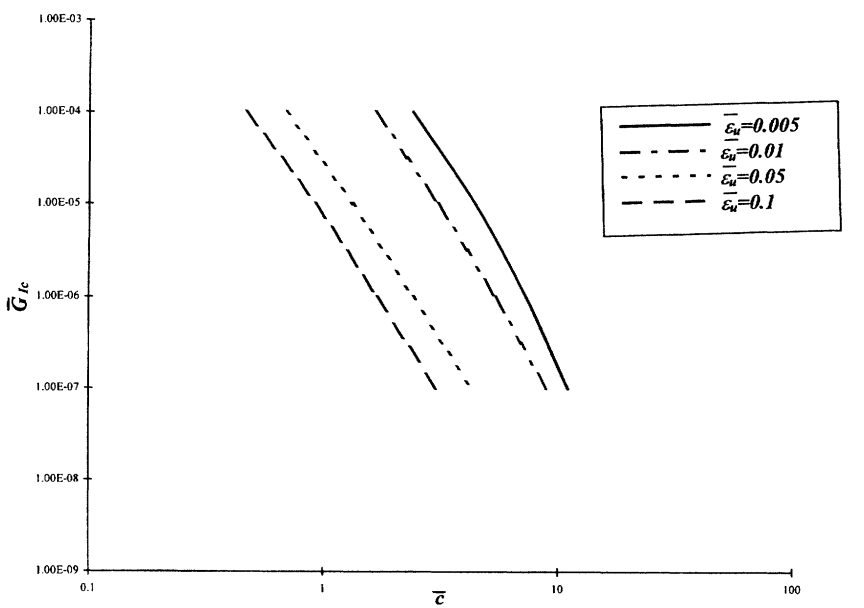

Figure 14. *$\log(\overline{c}) - \log(\overline{G}_{Ic})$ plot showing effects of $\overline{G}_{Ic}$ on $\overline{c}$.*

Downloaded from http://jcm.sagepub.com at UNIV OF FLORIDA Smathers Libraries on May 26, 2009

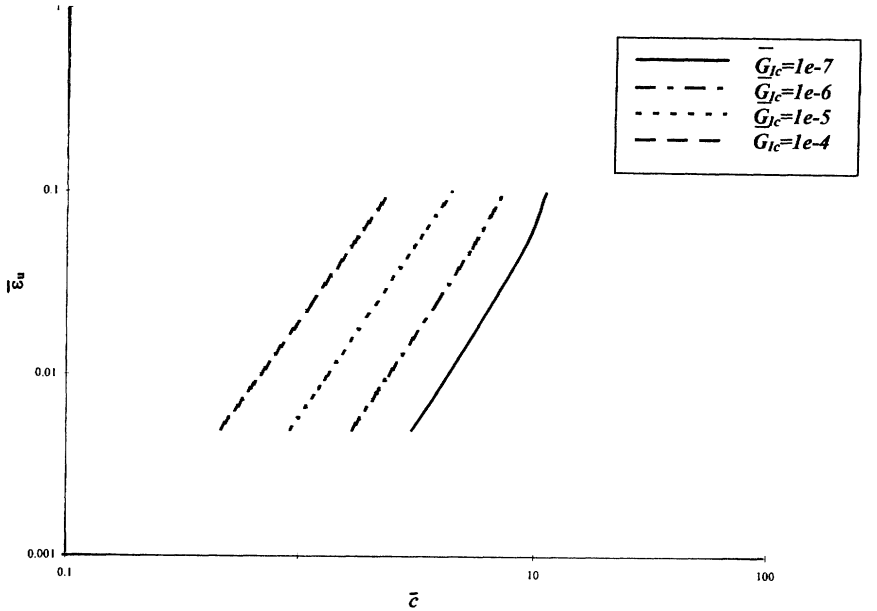

Figure 15. $\log(\bar{c}) - \log(\bar{\varepsilon}_u)$ *plot showing effects of* $\bar{\varepsilon}_u$ *on* $\bar{c}$.

most of the runs considered, except for the case considered in Figures 8 through 10. From the log-log plots an semi-empirical formula was derived for the bridging length as:

$$\bar{c} = c/h = 0.76 \frac{\sqrt{\bar{\varepsilon}_u}}{\bar{G}_{Ic}^{1/4}} \tag{25}$$

This formula has also been verified using Rayleigh-Ritz method (Appendix II).

6.6 Comparison with Experimental Results

The model described in this paper was used to estimate the fracture toughness in two examples for which test results are available in Sharma and Sankar [3]. In these examples, AS4/3501-6 unidirectional graphite/epoxy laminates were stitched with glass and Kevlar yarns. The results are summarized in Table 3. The properties for the stitch yarn in the table were taken from Williams [9]. The Mode I fracture toughness of the graphite/epoxy laminate was measured to be 300 J/m^2. First, the apparent fracture toughness was computed using Equation (15), and the results are given under the column 7 of Table 3. As seen from the table the results

Downloaded from http://jcm.sagepub.com at UNIV OF FLORIDA Smathers Libraries on May 26, 2009

Table 3. Elastic and plastic fracture properties of various stitch yarns.

Yarn	Denier (gm/9000 m)	ρ (Kg/m^3)	E (Gpa)	NSPSM	h (mm)
Kevlar	1600	1440	130	24,800	1.84
Glass	5952	2490	72	24,800	2.15

Yarn	Breaking Strength	G_{Ic-app} (Elastic)	ε_p	G_{Ic-app} (Plastic)	Exptl.
Kevlar	347	680.235	0.07	4421	4500
Glass	1222	8323.85	—	—	7800

are in good agreement for the glass yarn, but grossly under-estimates the effect of Kevlar stitches. One reason could be that the load-deflection behavior of Kevlar yarns are highly non-linear, and they can undergo large strains before failure. A simple model for yarns that undergo nonlinear behavior will be an elasto-plastic model. If the ultimate strain is much larger, then a fully plastic model will also be a good approximation. In that case, the fracture toughness of the stitched laminate (Equation 23) can be modified as

$$G_{Ic-max} = G_{Ic} + 2A_f h\sigma_u \varepsilon_u \tag{26}$$

where, σ_u is the ultimate strength and ε_u is the ultimate strain. Assuming $\varepsilon_p = 0.07$ for Kevlar the apparent fracture toughness is calculated to be 4421 J/m^2, which is closer to the experimental value of 4500 J/m^2. The load-deflection diagrams generated from this model (Figures 5, 8, and 11) compare very well with the experimental results of Dexter and Funk [2].

6.7 Debonding of Stitches

An estimate of energy required to debond the stitches from the parent laminate can be easily made from the disbond area and the Mode II Fracture Toughness. The disbond area for each stitch will be equal to the product of the circumference of the stitch cross-section and the laminate thickness. Then, from the number of stitches per unit area of the laminate, we can compute the contribution of stitch debonding to the fracture toughness. It is assumed that the stitch debonding is a pure Mode II fracture process, and the fracture toughness can be estimated as 670 J/m^2 [3]. For the material properties listed in Table 3, this contribution was estimated to be 17.977 J/m^2 and 4.426 J/m^2 respectively for the Glass and Kevlar yarns. It may be noted that this is not significant compared to the energy required

Downloaded from http://jcm.sagepub.com at UNIV OF FLORIDA Smathers Libraries on May 26, 2009

to break the stitches. Hence the error in the present model is expected to be negligible.

7. CONCLUSIONS

A simple analytical model has been developed for simulating the load-deflection behavior of stitched double cantilever beam specimens. A simple method has been proposed to compute the strain energy release rate due to delamination in stitched beams. The method is verified by the simulations performed using the present model. It is found that the maximum attainable increase in fracture toughness can be easily computed by the energy absorbed by the stitches in the breaking process. The crack bridging length behind the crack tip varies with the stitch parameters. A closed form expression has been derived for the non-dimensional crack bridging length in terms of the fracture toughness of the parent laminate and the ultimate strength of the stitches.

ACKNOWLEDGEMENTS

The funding for this research was provided by the Florida Space Grants Consortium and the Technological Research and Development Authority of the State of Florida.

APPENDIX I

The equations in $a_1 \ldots a_4$ that correspond to each boundary condition are given below:

$$\text{at } x = c,\ \psi = 0; \quad \sum_{i=1}^{4} a_i e^{\lambda_i c} = 0 \tag{A1}$$

$$\text{at } x = c,\ w = 0; \quad \sum_{i=1}^{4} \frac{a_i e^{\lambda_i c}}{r_i} = 0 \tag{A2}$$

$$\text{at } x = 0,\ V = -F: \quad \sum_{i=1}^{4} \left(\frac{r_i + \lambda_i}{r_i} \right) a_i = \frac{-F}{GA} \tag{A3}$$

$$\text{at } x = 0,\ M = -C: \quad \sum_{i=1}^{4} a_i \lambda_i = \frac{-C}{EI} \tag{A4}$$

Downloaded from http://jcm.sagepub.com at UNIV OF FLORIDA Smathers Libraries on May 26, 2009

APPENDIX II

Assume the beam deflection to be of the form:

$$w(x) = \alpha x^2 + \beta x^3 + \gamma x^4 \tag{A5}$$

The strain energy in the beam is given by:

$$U = \int_0^c \frac{EI\,(w'')^2\,dx}{2} + \frac{1}{2}\int_0^c kbw^2 dx \tag{A6}$$

External potential energy is:

$$V = -Pw(c) - C\left.\frac{dw}{dx}\right|_{x=c} \tag{A7}$$

Total potential energy in the beam is:

$$\Pi = U + V \tag{A8}$$

Substituting from Equation (A5) for $w(x)$ into Equation (A8) and minimizing Π with respect to α, β and γ we obtain three equations in α, β and γ.

$$\begin{bmatrix} 4+\frac{\kappa}{5} & 6+\frac{\kappa}{6} & 8+\frac{\kappa}{8} \\ 6+\frac{\kappa}{6} & 12+\frac{\kappa}{7} & 18+\frac{\kappa}{8} \\ 8+\frac{\kappa}{7} & 18+\frac{\kappa}{8} & \frac{144}{5}+\frac{\kappa}{9} \end{bmatrix} \begin{Bmatrix} \alpha c^2 \\ \beta c^3 \\ \gamma c^4 \end{Bmatrix} = \begin{Bmatrix} 2 \\ 3 \\ 4 \end{Bmatrix} \frac{Cc^2}{EI} \tag{A9}$$

where, $\kappa = k^{c4}/EI$. For small values of κ, using MATLAB to solve Equation (A9), we obtain the maximum strain in the stitches and the SERR as

$$\varepsilon_{max} = \varepsilon_u = \frac{1}{2}\frac{Cc^2}{EIh} \tag{A10}$$

$$G_I = G_{Ic} = \frac{C^2}{bEI} \tag{A11}$$

Downloaded from http://jcm.sagepub.com at UNIV OF FLORIDA Smathers Libraries on May 26, 2009

Note that in Equations (A10) and (A11) we have used the fact that at the instant of crack propagation, $\varepsilon_u = \varepsilon_{max}$ and $G_I = G_{Ic}$.

Eliminating C from Equations (A10) and (A11) and rearranging we get,

$$\bar{c} = 0.76 \frac{\sqrt{\bar{\varepsilon}_u}}{\bar{G}_{Ic}^{1/4}} \tag{A12}$$

It may be noted that $\bar{c}$ in Equation (A12) is the same as obtained by numerical simulation [*cf.* Equation (25)].

REFERENCES

1. Mignery, L.A., Tan, T.M. & Sun, C.T., 1985. "The use of stitching to suppress delamination in laminated composites," *ASTM STP 876, American Society of Testing Materials,* Philadelphia, USA, pp. 371–385.
2. Dexter, H.B. & Funk, J.G., 1986. "Impact resistance and Interlaminar fracture toughness of through-the-thickness reinforced graphite-epoxy." *AIAA paper 86-CP.*
3. Sankar, B.V. & Sharma, K.S., 1995. "Effects of through-the-thickness stitching on impact and interlaminar fracture properties of textile graphite/epoxy laminates." *NASA CR-195042.* NASA Langley, Hampton, VA.
4. Jain, L.K. & Mai, Y-W., 1994. "On the effect of stitching on Mode I delamination toughness of laminated composites." *Comp. Sci. & Technol., 51.* pp. 331–345.
5. Dransfield, K., Baillie, C.A. & Mai, Y-W., 1994. "Improvement of Delamination resistance in CFRP by stitching—A review." *Comp. Sci. & Technol. 50.* pp. 331–345.
6. Chen, V.L., Wu, X.X. & Sun, C.T., 1993. "Effective Interlaminar Fracture Toughness in Stitched Laminates." *Proceedings of the 8th Annual Technical Meeting of the American Society of Composites.* Cleveland, OH. pp. 453–462.
7. Sankar, B.V., 1991. "A finite element for modeling delamination in composite beams." *Computers & Structures, 38, No. 2,* pp. 239–246.
8. Sankar, B.V. & Sonik, V., 1997. "Pointwise Energy Release Rate in Delaminated Plates." *AIAA, 33, No. 7.*
9. Williams, J.G., 1985. "Fiber Systems" Chapter 3, *Composite Materials for Aircraft Structures.* Hoskin, B.S. & Baker, A.A., Eds., *AIAA Education Series.*
10. Ogo, Y., 1987. "The effect of stitching on in-plane and interlaminar properties of carbon fiber/epoxy fabric laminates." MSc. thesis, University of Delaware. Delaware.
11. Pelstring, R.M. & Madan, R.C., 1989. "Stitching to improve damage tolerance of composites.", *34th International SAMPE Symposium.*
12. Shu, D. & Mai, Y-W., 1993. "Effect of Stitching in Interlainar delamination extension in composite laminates." *Comp. Sci. & Technol. 49.* pp. 165–171.
13. Su, K.B. 1989. "Delamination Resistance of stitched thermoplastic matrix composite laminates." *Advances in Thermoplastic Matrix composite materials,* ed. F.M. Newaz. ASTM STP 1044. American Society of Testing Materials, Philadelphia, USA, pp. 279–300.
14. Ye, L., 1992. "Evaluation of Mode I interlaminar fracture toughness for fiber-reinforced composite materials for fiber-reinforced composite materials." *Comp. Sci. & Technol. 43.* pp. 49–54.
15. Etter, D.M. "Structured FORTRAN 77 for Engineers and Scientists." 2nd ed., *The Benjamin/Cummings Publishing Company Inc.*

Downloaded from http://jcm.sagepub.com at UNIV OF FLORIDA Smathers Libraries on May 26, 2009